Thin-Walled Structures 49 (2011) 304–316

Contents lists available at ScienceDirect

Thin-Walled Structures

journal homepage: www.elsevier.com/locate/tws

Buckling of thin and moderately thick anisotropic cylinders under combined torsion and axial compression

Atsushi Takano

Mechanical Engineering Section, Space Systems Department, Kamakura Works, Mitsubishi Electric Corporation, 325 Kamimachiya, Kamakura, Kanagawa 247-8520, Japan

ARTICLE INFO

Article history:
Received 2 November 2009
Received in revised form
1 November 2010
Accepted 1 November 2010
Available online 20 November 2010

Keywords:
Buckling
Shell
Anisotropy

ABSTRACT

The effects of anisotropy, transverse shear stiffness, length, and their interactions on buckling under pure torsion and under combined axial compression and torsion were investigated using a previously derived analytical model based on deep shell theory including anisotropy and transverse shear stiffness. The model was verified only for buckling under pure axial compression, hence results for buckling under torsion have now been compared with the results of previous analyses, and the comparison showed that the model has good accuracy for buckling under torsion. Investigation showed that the buckling loads of a cylindrical shell are affected not only by anisotropy and transverse shear stiffness but also by shell length. This means that the shallow shell theory (Donnell-type theory) is not appropriate and deep shell theory including anisotropy and transverse shear stiffness must be used.

1. Introduction

Many studies analyzing the buckling of orthotropic or anisotropic circular cylindrical shells have been reported in the past few decades [1–21], but none were based on deep shell theory, which can account for the effects of length, including both layup anisotropy and transverse shear stiffness. Booton and Tennyson [21] analyzed the buckling of anisotropic cylinders under pure torsion and combined torsion and axial compression but did not consider the interaction between length and anisotropy because their analysis was based on Donnell's theory, which cannot account for the effect of length. Ho and Cheng [10] reported results of buckling under torsion, external pressure, and combined torsion and external pressure that were obtained using Flügge's deep shell theory including only the effect of anisotropy. They did not report results for the interaction between anisotropy and length. One analysis took into account the effect of transverse shear stiffness [22], but the effect of length and anisotropy was not considered because the analysis was based on Donnell's theory.

In the work reported here, the ways that buckling of thin and moderately thick cylinders under pure torsion and under combined axial compression and torsion is affected by the interactions between anisotropy and length and between transverse shear stiffness and length were investigated. The analytical model used in such an investigation must be based on deep shell theory and first-order shear deformation theory including layup anisotropy and transverse shear stiffness. Such a model has been described [23], but it was verified for only axial buckling. This paper therefore begins by showing that the model can also apply to torsional buckling loads.

Fiber-reinforced-plastic and honeycomb-sandwich cylindrical shells generally have small transverse shear stiffness in spite of their thin walls. Such cylinders with small transverse shear stiffness must thus be modeled by first-order shear deformation theory. Of course, moderately thick cylinders must also be modeled by first-order shear deformation theory. Thick and very thick cylinders, which require the use of higher-order shear deformation theories, are not discussed in this paper because such cylinders collapse due to material failure, not buckling.

2. Validation for torsional buckling

Consider a circular cylindrical shell with thickness t, radius r, and length l that is made of a laminate consisting of orthotropic layers of uniform thickness bonded together perfectly. Axial compression per unit length, P, and torsional (shearing) force per unit length, T, are applied to the shell. The coordinate system and notation are shown in Fig. 1.

The material properties of the carbon fiber reinforced plastic (CFRP) prepreg and the honeycomb core considered here are listed in Table 1, and the specifications of the layups treated are listed in Tables 2 and 3. Note that high-modulus CFRP prepregs like those listed in Table 1 are often used in spacecraft. The simply supported condition, $v = w = N_x - Pu_{,x} - Tu_{,\theta}/r = M_x = M_{x\theta} = 0$, is used throughout this paper.

Numerical examples are compared with results from previous analyses [22,24,25] to verify the analytical model (Eq. (A.18) in Appendix A) derived previously [23] for torsional buckling. This model is based on Cheng and Ho's equations [9], which are based on

E-mail address: Takano.Atsushi@dr.MitsubishiElectric.co.jp

0263-8231/$ - see front matter © 2010 Elsevier Ltd. All rights reserved.
doi:10.1016/j.tws.2010.11.001

Nomenclature

A_{ij}	in-plane stiffness
A^*_{ij}	$1/a^*_{ij}$
$[a^*]$	$[A]^{-1}$, in-plane compliance
a_{ij}	normalized in-plane stiffness
B_{ij}	extensional/flexural coupling
b_{ij}	normalized extensional/flexural coupling
c_{ij}	shear correction factor
D_{ij}	flexural stiffness
d_{ij}	normalized flexural stiffness
G	"geometric stiffness" matrix [Eq. (A.13)]
G_{ij}	shear modulus
K	"stiffness" matrix [Eq. (A.13)]
K_c	normalized axial load factor
K_T, K_{Tshell}	normalized torsional load factor
l	length of cylindrical shell
m	number of half-waves in axial direction
M_x, M_θ, $M_{\theta x}$, $M_{x\theta}$	moment resultants per unit length
n	number of waves in circumferential direction
N_x, N_θ, $N_{\theta x}$, $N_{x\theta}$	in-plane force resultants per unit length
P	external axial compression per unit length
P_{cr}	buckling load under pure axial load
$\overline{Q}_{ij}$	transformed reduced stiffness
q_2, q_3	load parameters
R	radial coordinate
R_C	P/P_{cr}
R_T	$T/\lvert T^-_{cr}\rvert$
r	radius of cylindrical shell
S_{ij}	transverse shear stiffness
s_{ij}	normalized transverse shear stiffness
T	external torsional force per unit length
T^-_{cr}	torsional buckling load under pure negative torsional load
$T_{crimping}$	torsional crimping load
T_{NASA}	torsional buckling load based on NASA's design criteria
$T_{plate\text{-}strip}$	shear buckling load of a plain plate strip
t	thickness of cylindrical shell
u, v, w	middle surface displacements in x, θ, and z directions
U, V, W, Γ_x, Γ_θ	displacement amplitudes
x	axial coordinate of middle surface
Z	$l^2/(r\times t)$
z	radial coordinate of middle surface
δ_D, γ_D	flexural-twist anisotropy factors
γ_x, γ_θ	rotation of lines normal to middle surface
λ	$m\pi r/l$
θ	circumferential coordinate of middle surface

Flügge's deep shell theory including layup anisotropy and are improved by using first-order shear deformation theory. Thus, if the transverse shear stiffness used is large enough, the numerical results obtained using this model should match the results of Cheng and Ho's equations. Cheng and Ho's numerical results (Figs. 9–11 of Ref. [10]) can be easily obtained for anisotropic cylindrical shells by using Eq. (A.18). Thus, the model is obviously validated for the torsional buckling of anisotropic cylindrical shells.

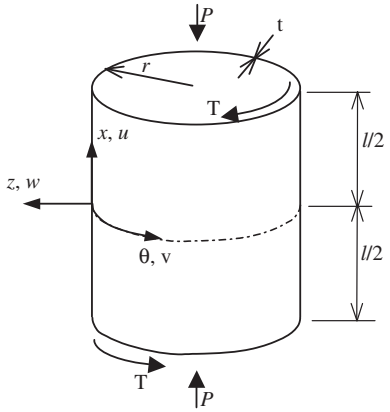

Fig. 1. Shell geometry and notation.

Table 1
Material properties.

Property	Value
CFRP prepreg (60 ton-class high modulus fiber)	
E_{11}	380,000 MPa
E_{22}	6000 MPa
G_{12}	4000 MPa
ν_{12}	0.33
Honeycomb core	
$G_{13}=G_{23}$	120 MPa

Furthermore, the torsional buckling loads were calculated using Eq. (A.18) over a wide range of lengths and compared with the results of previous analyses [22,24,25]. The results for circular cylindrical shells with a radius of 597 mm and made of laminated CFRP 3 mm thick ($r/t=199$) and 9.95 mm thick ($r/t=60$) are shown in Figs. 2a and b. The layup analyzed was layup B, which has small flexural/twist couplings D_{16} and D_{26} (Table 2). The effect of transverse shear stiffness was investigated by using two different values of transverse shear stiffness: $G_{13}=G_{23}=4000$ MPa and $G_{13}=G_{23}=4\times10^7$ MPa (which can be regarded as infinite). Usually, G_{13} and G_{23} are not assumed to be equal, but to enable the numerical results to be compared with Stein and Mayers' crimping load [22], here it is assumed that G_{13} and G_{23} are equal. To take the transverse shear deformation into account, first-order shear deformation theory and a shear correction factor are used. The first-order shear deformation theory with a shear correction factor has been shown to have good accuracy by comparing it with a higher-order shear deformation theory [26,27]. Shear correction factors $c_{11}=c_{22}=5/6$ and $c_{12}=0$ were used.

The normalized torsional load factor is defined as

$$K_T=\frac{T}{(D_{11}D_{22})^{1/2}/(rt)}. \tag{1}$$

The solution should be close to the buckling load of a plane plate strip [24] or crimping [22] when l/r is small and close to the torsional buckling load of a long rod when l/r is large. Hence, for comparison with the buckling load of a plane plate strip, the load factor is plotted against $(l/r)\times(r/t)^{1/2}$ in Fig. 2a. For comparison with the torsional buckling load of a long rod, it is plotted against $(l/r)/(r/t)$ in Fig. 2b.

As shown in Fig. 2a, when $(l/r)\times(r/t)^{1/2}$ is small, the curves calculated considering the effect of transverse shear deformation ($G_{13}=G_{23}=4000$ MPa) approach the curves of crimping load. The crimping load [22] is given by

$$T_{crimping}=c_{ii}S_{ii}, \tag{2}$$

when $c_{11}S_{11}=c_{22}S_{22}=c_{ii}S_{ii}$ and $c_{12}S_{12}=0$. The crimping load factors are shown on the left-hand side of Fig. 2a.